Ultraviolet photoelectron spectroscopy of molybdenum and molybdenum monoxide anions

Robert F. Gunion, St. John Dixon-Warren, and W. Carl Lineberger
JILA and Department of Chemistry and Biochemistry, University of Colorado, Boulder, Colorado 80309-0440

Michael D. Morse
Department of Chemistry, University of Utah, Salt Lake City, Utah 84112

The 351 nm photoelectron spectra of Mo^- and MoO^- have been measured. The electron affinity of atomic molybdenum is 0.748(2) eV and that of molybdenum monoxide is 1.290(6) eV. The term energies of several MoO electronic states not previously observed are obtained and compared with *ab initio* predictions. The ground state of MoO is confirmed to have $^5\Pi$ symmetry and the term energy of the $^3\Pi$ excited state, 10 179(20) cm^{-1}, closely matches calculations. The ground state of MoO^- is a $^4\Pi$ state with a vibrational frequency of 810(40) cm^{-1}. The first excited state of molybdenum monoxide is tentatively assigned as a $^3\Delta$ state with $T_0 = 621(50)$ cm^{-1}. At least one state, possibly a $^5\Sigma^-$ state, lies 8000(500) cm^{-1} above the ground state, and a $^5\Sigma^+$ state is observed at 11 590(60) cm^{-1} above the ground state. The separations of spin–orbit levels for the MoO X $^5\Pi$, $^3\Pi$, and $^3\Delta$ states are 169(30), 410(20), and $-720(20)$ cm^{-1}, respectively. The vibrational frequencies of the $^3\Pi$ and $^3\Delta$ states are found to be 600(20) and 1000(20) cm^{-1}, respectively. These observations give new insight into the Mo–O bond. © *1996 American Institute of Physics.* [S0021-9606(96)00205-3]

I. INTRODUCTION

Transition metal oxides are ubiquitous in environments as diverse as interstellar media,[1] surface chemistry, and as superconducting materials. The presence of many unpaired electrons in *d* orbitals gives rise to a wide variety of low-lying electronic states, even in the diatomics, making both experiments and calculations unusually challenging. Molybdenum monoxide illustrates these difficulties especially well, since the molybdenum atomic ground state has six unpaired electrons in a $5s^1 4d^5$ configuration. Low-lying states of MoO have been theoretically predicted[2,3] with spin multiplicities ranging from $S = 1$ (triplets) to $S = 3$ (septets). The MoO low-lying electronic states have spin multiplicities at least as high as triplets, and quintets and septets are common. Negative ion photoelectron spectroscopy provides a unique opportunity to study otherwise inaccessible electronic states of MoO because, with a quartet ground state in the anion, transitions to both triplet and quintet states are fully allowed, and because the energy range available, from 0 to 3.5 eV above the anion ground state, is not easily probed by other methods.

Experimental observations of the MoO electronic states are sparse, largely because MoN has proven[4] to be a major contaminant in the generation of MoO. The first MoO emission spectrum was taken in 1933 by Picardi.[5] In 1957, the Vatican City Atlas[6] reported 20 MoO emission bands from 11 549 to 16 690 cm^{-1}; however, 14 of these were subsequently attributed[7] to $Mo_x N$. Huber and Herzberg's comprehensive 1979 compilation of diatomic constants[8] lists only a dissociation energy for the ground state, and several unidentified bands from the Vatican City Atlas reference. Also in 1979, Bates and Gruen[9] published a matrix study of MoN,

MoO, and Mo_2; the primary information obtained for $Mo^{16}O$ was the ground state vibrational frequency at 893.5 cm^{-1}. A 1991 REMPI study of MoO by Hamrick *et al.*,[4] where the MoN contamination was overcome by use of a jet-cooled molecular source, represents the only conclusive study to date of the excited electronic states between 11 300 and 22 000 cm^{-1}. Among the findings in this latest report is the identification of the ground state symmetry of MoO as $^5\Pi$, with a positive spin–orbit coupling such that the $^5\Pi_{-1}$ level lies at lowest energy.

The majority of work done on MoO has been theoretical. Bauschlicher and co-workers address[2,10,11] the term energies and spectroscopic constants of MoO and other transition metal oxides at various levels of *ab initio* theory. The first study[10] found that MoO, CrO, NiO, PdO, and AgO all display significant ionic character. The second[11] compares WO with CrO and MoO. The final paper (Langhoff *et al.*[2]) presents MCPF and CASSCF/MRCI results for the oxides and sulfides of molybdenum and technetium, including seven of the lowest triplet, quintet, and septet electronic states of MoO. The first excited state was found to be $^3\Delta$; using varying levels of theory and basis sets the term energy of this state ranged[2] from 2007 to 5635 cm^{-1}. Brocławik and Salahub[3] employed spin-polarized density functional calculations to examine ten MoO states (triplets, quintets, and septets); term energies for the $^3\Delta$ state using this method varied from 2193 to 3265 cm^{-1}. The ground state of MoO was consistently[2,3,10,11] found to be a $^5\Pi$ state, with the configuration $2\delta^2 12\sigma^1 6\pi^1$. Brocławik[12] also calculated the ground state of MoO^- as a $^4\Pi$ state, in accord with the data presented here.

This report is organized as follows: The method of nega-

tive ion photoelectron spectroscopy will be described briefly first, followed by the Mo^- photoelectron spectrum. The analysis of the MoO^- spectrum will be covered next, starting with a brief qualitative description of the electronic configurations of MoO and MoO^-, followed by an overview of the experimental results, photoelectron angular distribution measurements, and estimates of spin orbit coupling parameters of some MoO electronic states. The photoelectron spectrum of MoO^- will be assigned next by discussing the $X\ ^5\Pi$ state first, then the $^3\Pi$ and $^3\Delta$ states, and finally the $^5\Sigma^+$ and $^5\Sigma^-$ states. Comments about the electronic structure and bonding properties of MoO as they are currently understood conclude this study.

II. EXPERIMENTAL DETAILS

The photoelectron spectrometer has been described in detail previously[13,14] and more concisely in a recent review.[15] Molybdenum atomic anions and molybenum monoxide anions were created downstream of a microwave flowing afterglow ion source by adding molybdenum hexacarbonyl into the flowing helium buffer gas (6 standard liters per minute) with trace oxygen (5 standard cm^3 per minute). Total pressures in the flow tube were approximately 0.5 Torr. Typical ion currents were 6 pA for the atomic anion and 15 pA for the oxide; temperatures of ions formed in this source are typically 300–350 K. The ions were then accelerated to 735 eV, mass-selected in a Wien filter, and decelerated to 40 eV prior to passing through an interaction region perpendicular to the path of a fixed-frequency, cw argon ion laser operating at 351 nm. Electrons detached within a small solid angle passed through a hemispherical electron energy analyzer. Typical electron energy resolution is 6 meV. The electron kinetic energy scale was calibrated to the atomic oxygen electron affinity[16] to fix the absolute electron kinetic energy scale, and a correction for the energy scale compression was made using the known tungsten electron affinity and term energies.[17] The electron binding energy used throughout this report is obtained by subtracting the electron kinetic energy from the photon energy (3.5311 eV).

III. ATOMIC MOLYBDENUM

While the focus of this report is on MoO^-, the Mo^- photoelectron spectrum provides useful information for making the MoO^- spectral assignments. For this reason and the fact that it represents an improvement over the previous photoelectron spectrum from this laboratory,[18] the atomic molybdenum spectrum is presented first, followed by analysis of the MoO^- spectrum.

Figure 1(a) shows the 351 nm photoelectron spectrum of Mo^-. The two prominent peaks correspond to s-electron detachment from the $Mo^-\ a\ ^6S_{5/2}$ state to the labeled neutral states. The binding energy of the single peak at low binding energy, which results from transitions to the $a\ ^7S_3$ state, provides one determination of the adiabatic electron affinity, 0.750(6) eV. Another prominent peak at 2.081 eV electron binding energy corresponds to a transition producing the $^5S_2$ state, and transitions to several spin orbit states in the
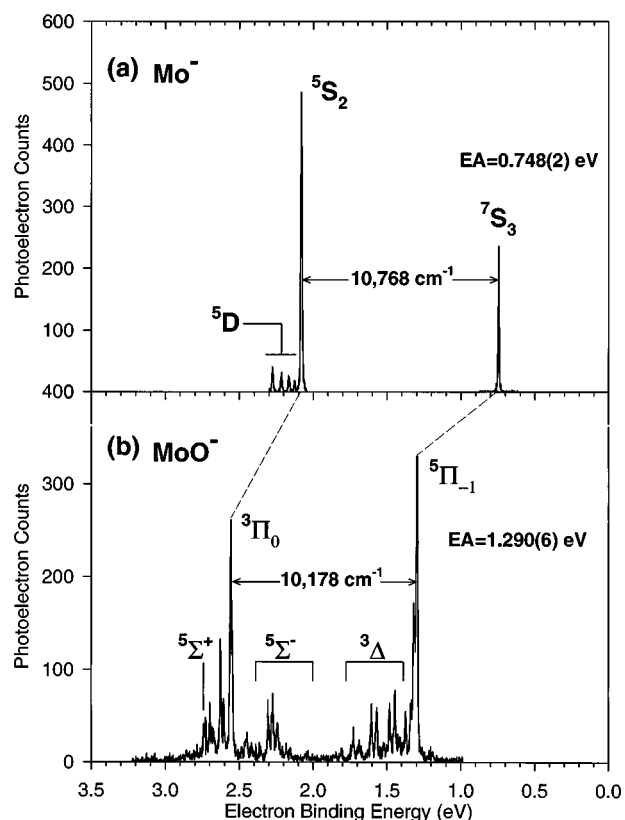

FIG. 1. 351 nm photoelectron spectra of (a) Mo^-, showing transitions to the $^7S_3$, $^5S_2$, and $^5D_\Omega$ (Ω=1,2,3,4) neutral atom states from $Mo^-\ ^6S_{5/2}$, and (b) MoO^-, showing general positions of neutral MoO states observed. The splitting between the Mo $^7S_3$ and $^5S_2$ states, and the MoO $^5\Pi_{-1}$ and $^3\Pi_0$ states, is also indicated for comparison.

^5D manifold appear as minor peaks between 2.126 and 2.276 eV binding energy. Comparison of all of these measured peak positions with those listed by Moore[17] provides a more accurate determination of EA(Mo) to be 0.748(2) eV, an improvement on the previously measured value[18] of 0.747(10) eV.

Special note should be taken of the fact that the two prominent peaks in the Mo^- photoelectron spectrum correspond to photodetachment of an electron from the fully occupied $5s$ orbital, leaving the other electron either high spin ($^7S_3$) or low spin ($^5S_2$) coupled to the $4d$ electrons. The cross section for photodetachment from a $4d$ orbital is much lower than from a $5s$ orbital, as is apparent in the low intensities of the ^5D transitions relative to the $^7S_3$ and $^5S_2$ peaks in Fig. 1(a). This dominance of s-electron photodetachment will greatly assist the interpretation of the MoO^- spectrum, to be discussed next.

IV. MOLYBDENUM MONOXIDE

A. Electronic structure

The photoelectron spectrum of MoO^- is most easily understood with the aid of the correlation diagram shown in Fig. 2 for the MoO $X\ ^5\Pi$ configuration. The ground state configurations of the separated atoms are illustrated on either
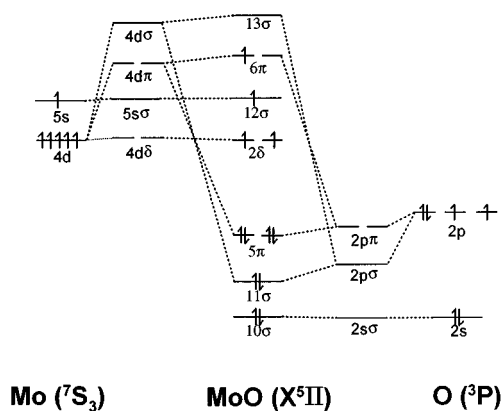
FIG. 2. Correlation diagram for molybdenum monoxide, derived from the Mo and O atoms.

TABLE I. Dominant configurations of the MoO^- and MoO electronic states discussed in the text. Orbital designations are consistent with Fig. 2. Adapted from Refs. 2 and 3.

	Electronic state	Configuration[a]
MoO^-	$^4\Pi$	$11\sigma^2 5\pi^4 2\delta^1 2\overline{\delta}^1 12\sigma^2 6\pi^1$
MoO	$^5\Pi$	$11\sigma^2 5\pi^4 2\delta^1 2\overline{\delta}^1 12\sigma^1 6\pi^1$
	$^3\Delta$	$11\sigma^2 5\pi^4 2\delta^2 2\overline{\delta}^1 12\sigma^1$
	$^5\Sigma^+$	$11\sigma^2 5\pi^4 2\delta^1 2\overline{\delta}^1 6\pi^1 6\overline{\pi}^1$
	$^3\Pi$	$11\sigma^2 5\pi^4 2\delta^1 2\overline{\delta}^1 12\sigma^1 6\pi^1$
	$^5\Sigma^-$	$11\sigma^2 5\pi^4 2\delta^1 2\overline{\delta}^1 12\sigma^1 13\sigma^1$
	$^3\Sigma^-$	$11\sigma^2 5\pi^4 2\delta^1 2\overline{\delta}^1 12\sigma^2$

[a]The 11σ and 5π orbitals denote the (Mo $4d\sigma$+O $2p\sigma$) and (Mo $4d\pi$+O $2p\pi$) bonding orbitals, respectively; the 13σ and 6π orbitals are the antibonding counterparts. The 2δ and 12σ nonbonding orbitals derive from the Mo $4d\delta$ and $5s\sigma$ orbitals, respectively.

side of Fig. 2 and the MoO X $^5\Pi$ state configuration appears in the center. The ordering of the orbitals is consistent with approximations of the orbital energies made by Hamrick *et al.*[4] As the Mo and O atoms approach from large internuclear distances, an ionic interaction (Mo^+O^-) splits the valence atomic orbitals: the Mo $4d$ orbitals split into a σ, two π, and two δ orbitals; similarly the oxygen $2p$ orbitals split into σ and π components. The localization of negative charge on the oxygen atom destabilizes the molybdenum $4d$ orbitals, affecting the $4d\sigma$ orbital most strongly and the $4d\delta$ orbital least. The attraction of the oxygen $2p$ orbitals to the positively charged metal atom stabilizes the orbitals; again the σ orbital is most strongly affected by the internuclear forces. The Mo $5s\sigma$ orbital is largely unperturbed by the oxygen atom and remains essentially nonbonding.

As the atoms continue to approach, a covalent interaction becomes important and the orbitals mix into molecular orbitals of similar symmetry (O $2p\sigma$+Mo $4d\sigma$, and O $2p\pi$ +Mo $4d\pi$). The resulting bonding orbitals (the 11σ and 5π orbitals, Fig. 2) are fully occupied in the low-lying MoO electronic states, and antibonding partners to these orbitals are the 6π and 13σ orbitals. The Mo $4d\delta$ and $5s\sigma$ orbitals remain nonbonding, forming the 2δ and 12σ orbitals. The ground state electron configuration of MoO is shown in Fig. 2, where one unpaired electron resides in each of the three nonbonding orbitals and one more is in the 6π antibonding orbital. The Mo–O bond, therefore, consists of the fully occupied 5π and 11σ bonding orbitals and the singly occupied 6π antibonding orbital for a formal bonding order of 2.5.

From this orbital description of MoO, the orbital in which the extra electron in MoO^- will reside can be predicted straightforwardly: the electron–electron repulsion energy generated by inserting a second electron in one of these orbitals will be minimized for the large 12σ (essentially Mo $5s$) orbital relative to the orbitals derived from the more compact Mo $4d$ orbitals. The ground state of MoO^-, therefore, will be the $2\delta^1 2\overline{\delta}^1 12\sigma^2 6\pi^1$, $^4\Pi$ state. This prediction is borne out by the assignments and angular distributions to be presented below.

The electron configurations of the MoO and MoO^- states observed in the MoO^- photoelectron spectrum are listed in Table I. The MoO ground state has been previously assigned experimentally[4] and through calculations.[2,3,10,11] The configurations given in Table I for the remaining states of the neutral are from Refs. 2 and 3. Some general notes can be made about the configurations in Table I before analyzing the spectrum: The MoO X $^5\Pi$ and $^3\Pi$ states differ only in a spin flip of the $12\sigma(5s\sigma)$ electron; the anion ground state is similar except that this orbital is doubly occupied. Removal of one of the 12σ electrons from the anion will produce either the $^5\Pi$ or the $^3\Pi$ state of the neutral, depending on whether the electron that remains is high- or low-spin coupled to the 2δ and 6π electrons. Therefore, if the anion ground state is the $^4\Pi$ state, transitions to the neutral $^5\Pi$ and $^3\Pi$ states would be expected to be very prominent. Also, since the electron is removed from a nonbonding orbital, the geometry change between the anion and neutral should be small, producing large Franck–Condon factors only for $\Delta v = 0$ transitions to either the $^5\Pi$ or the $^3\Pi$ state.

The remaining electronic state configurations in Table I are expected to have smaller cross sections for photodetachment from the anion ground state than the $^5\Pi$ and $^3\Pi$ states. Photodetachment transitions producing the $^3\Delta$, $^5\Sigma^-$, and $^5\Sigma^+$ states are two electron processes requiring both electron detachment and electronic excitation of the remaining core, significantly decreasing the probability for such a transition. Transitions to the $^3\Sigma^-$ state require only detachment of an electron, but it must come from the $4d\pi$ antibonding orbital. As seen in the Mo^- photoelectron spectrum, the cross section for photodetachment from a $4d$ orbital is much lower than from a $5s$ orbital and this process should also be relatively weak.

The molecular orbital picture presented in Fig. 2 and Table I provides a strong expectation for the appearance of the MoO^- photoelectron spectrum: Two major peaks, corresponding to transitions to the $^5\Pi$ and $^3\Pi$ states of MoO, should appear prominently. These peaks are to $v=0$ of the neutral, reflecting the small geometry change from the MoO^- X $^4\Pi$ state (at the approximately 300 K temperatures of our source); transitions to excited vibrational levels should not be overly apparent. The splitting between these two major peaks, equivalent to the energy required to flip the spin of

the 5s electron relative to the rest of the unpaired electrons, should be similar to the separation between the $^7S_3$ and $^5S_2$ states of atomic molybdenum. Finally, if transitions to any other MoO electronic states are apparent they should be weak compared to the $^5\Pi$ and $^3\Pi$ transitions.

B. Experimental results

The 351 nm photoelectron spectrum of MoO$^-$ is illustrated in Fig. 1(b). As in the Mo$^-$ spectrum, two sharp peaks separated by just over 10 000 cm^{-1} dominate the spectrum, in excellent agreement with the qualitative electronic structure considerations discussed above. Since the ground state of MoO is already known[2–4,10,11] to be the $^5\Pi$ state, the prominence of these two peaks confirms a $^4\Pi$ assignment for the anion ground state and strongly suggests that the peak near 2.5 eV binding energy corresponds to photodetachment into the MoO $^3\Pi$ state. Even more support for these assignments is found in the photoelectron angular distribution measurements described below. The adiabatic electron affinity of MoO is determined by the position of the lower binding energy peak at 1.290(6) eV, and the term energy of the $^3\Pi$ state is given by the spacing between the two prominent peaks (10 178 cm^{-1}).

Several smaller peaks appear in the MoO$^-$ spectrum, mostly grouped to the high binding energy side of the major peaks. The simple electronic structure arguments presented above are not sufficient to assign these peaks and so a more detailed analysis will be necessary. As a first step to this analysis, a few more preliminary observations can be made about the data depicted in Fig. 1(b): the features between 1 and 2 eV binding energy appear to result from transitions to a series of vibrational levels within the $^5\Pi$ state, albeit with an unusual Franck–Condon envelope. Further analysis will show that transitions to a second ($^3\Delta$) state are responsible for most of these peaks. The second set of peaks at 2.5 to 2.7 eV binding energy seems to be associated with the $^3\Pi$ state; and a third, smaller feature appears near 2.3 eV. The analysis to be presented below makes clear that vibrational progressions are not the only contributor to the smaller peaks. Additional information, available from angular distributions, spin orbit splittings, and calculations of term energies and vibrational frequencies, will be necessary in order to assign these features.

C. Photoelectron angular distributions

The dependence of photodetachment intensity on laser polarization produces essential additional information about the MoO states. The angular distribution of photoelectron detachment for a given transition is measured by varying the angle formed between the laser electric vector polarization and the electron collection direction. In the case of atomic photodetachment, the intensity of photoelectron detachment at a given angle θ is governed by the equation,[19–21]

$$I_\theta = 1 + \beta P_2(\cos\theta),$$

where $P_2(\cos\theta)$ is the second associated Legendre polynomial and β is an anisotropy parameter which can range over

$-1 \leq \beta \leq 2$. Since photons posess one unit of angular momentum, electrons which originate in atomic s orbitals result in p wave detachment and β is +2. Thus the (Mo $^7S_3$)$\leftarrow$(Mo$^-$ $^6S_{5/2}$) and (Mo $^5S_2$)$\leftarrow$(Mo$^-$ $^6S_{5/2}$) transitions display $\beta = 2$. Detachment of an electron from a p orbital will result in a combination of s wave and d wave detachment dependent on the electron kinetic energy: for photons near the threshold energy for photodetachment, s wave detachment will dominate, resulting in an isotropic distribution ($\beta = 0$); as photon energy is increased d wave detachment will gradually become more important and β will become negative for 1–2 eV photons. The anisotropy parameter for O$^-$ detachment as a function of photon energy has been measured by Hanstorp *et al.*[22] and a simple semiquantitative model presented. Similarly, electrons detached from d orbitals, such as the 4d orbitals in molybdenum, will display a mixture of p and f wave behavior; at electron kinetic energies below 1 or 2 eV, the p wave contribution dominates so that β is close to +2.

The interpretation of the anisotropy parameter in terms of the initially occupied orbital is more complicated in the molecular frame; however some trends have been observed in negative ion photoelectron spectra which allow limited interpretation of angular distributions: Electrons originating in large, diffuse σ orbitals display approximately p wave behavior so that β is between 1.5 and 2, while electrons which originate from π-type orbitals tend to produce angular distributions where $\beta < 0$ for electron kinetic energies in the range accessible with our experiment (0 to 3.5 eV). Detachment from d orbitals will tend to result in $\beta > 0$. Since the angular distributions evolve slowly as electron kinetic energy changes, the various vibrational levels in a given electronic state are expected to have similar angular distributions. Thus the angular distribution data may identify a vibrational progression in a complex spectrum, as well as provide a signal for the presence of an additional electronic state. Both of these circumstances will arise in the detailed analysis of the spectrum as reported below.

The spectra presented in Figs. 1, 3, and 4 were measured at the "magic angle" ($\theta = 54.7°$), where $P_2(\cos\theta) = 0$, resulting in a spectrum with relative peak heights independent of the angular distribution. Spectra of MoO$^-$ were also recorded at parallel ($\theta = 0°$) and perpendicular (90°) polarizations, from which the anisotropy parameter β was obtained for each of the observed peaks listed in Table II and labeled in Figs. 3 and 4. The anisotropy parameters of the X $^5\Pi$ origin (peaks A–C) and the $^3\Pi$ origin (peak Q) are close to +2, indicating that the electron is detached from a nearly spherical σ orbital in these cases. Since the 12σ orbital should be nearly unperturbed by the oxygen atom, the angular distribution provides strong evidence that the electron is detached from the 12σ orbital, confirming the assignment of the MoO$^-$ X $^4\Pi$ state. The only other peak to display a similarly large, positive anisotropy parameter is peak E, which will be assigned (Sec. IV E) to vibrational excitation of the MoO X $^5\Pi$ state. The intensities of the remaining peaks in the MoO$^-$ spectrum are much lower than the $^5\Pi$ and $^3\Pi$ state origins and therefore the anisotropy parameters
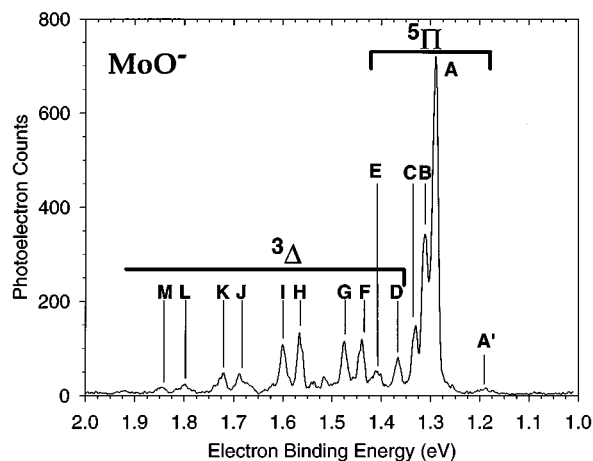
FIG. 3. Expanded view of MoO$^-$ photoelectron spectrum for electron binding energies between 1.0 and 2.0 eV. The energy of each transition is given in Table II.

are more difficult to obtain with the same degree of confidence. The measured values, which range between 0.4 and 1.2, are insufficient for assigning the peaks as transitions to separate electronic states based purely on angular distributions. While the smaller values show that the transitions are intermediate between σ orbital detachment and an isotropic distribution, some d orbital character is probably present in the orbitals; however, the degree of d orbital character is difficult to extract because the anisotropy parameters are not well determined. Assignments described below therefore rely on peak positions and relative intensities of the peaks, and comparisons with calculations and previous experiments, rather than on angular distributions.

D. Spin orbit splitting

The splittings between spin orbit levels in molybdenum monoxide are dominated by the characteristics of atomic molybdenum. The overall splitting ζ (defined by Blume and Watson[23]) of the atomic molybdenum $4d$ orbitals was calcu-
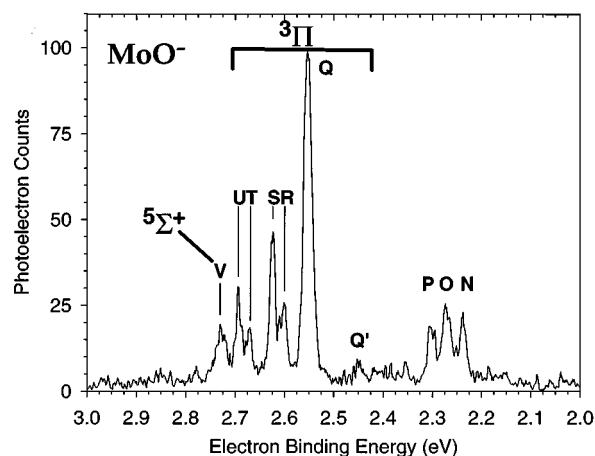

FIG. 4. Expanded view of MoO$^-$ photoelectron spectrum for electron binding energies between 2.0 and 3.0 eV. The energy of each transition is given in Table II.

TABLE II. Assignments, binding energies, and term energies for transitions observed in the MoO$^-$ 351 nm photoelectron spectrum. Peak labels are consistent with Figs. 3 and 4. All transitions originate in the MoO$^-$ $X\ ^4\Pi_{-1/2}(v=0)$ state.

Peak label	MoO state[a]	Electron binding energy (eV)	Term energy (cm^{-1})
A	$X\ ^5\Pi_{-1}(v=0)$	1.290	0
B	$X\ ^5\Pi_0(v=0)$	1.311	169
C	$X\ ^5\Pi_1(v=0)[^3\Delta_3/^5\Pi_3]$	1.331	331
D	$^3\Delta_3(v=0)[^3\Delta_3/^5\Pi_3]$	1.367	621
E	$X\ ^5\Pi_{-1}(v=1)$	1.409	960
F	$^3\Delta_2(v=0)[^3\Delta_3/^5\Pi_3]$	1.440	1210
G	$^3\Delta_3(v=1)[^3\Delta_3/^5\Pi_3]$	1.475	1492
H	$^3\Delta_2(v=1)[^3\Delta_3/^5\Pi_3]$	1.565	2218
I	$^3\Delta_3(v=2)[^3\Delta_3/^5\Pi_3]$	1.600	2500
J	$^3\Delta_2(v=2)[^3\Delta_3/^5\Pi_3]$	1.685	3186
K	$^3\Delta_3(v=3)[^3\Delta_3/^5\Pi_3]$	1.724	3500
L	$^3\Delta_2(v=3)[^3\Delta_3/^5\Pi_3]$	1.801	4121
M	$^3\Delta_3(v=4)[^3\Delta_3/^5\Pi_3]$	1.847	4493
N[b]	$[^5\Sigma^-]$	2.240	7662
O[b]	$[^5\Sigma^-]$	2.272	7920
P[b]	$[^5\Sigma^-]$	2.302	8162
Q	$^3\Pi_0(v=0)$	2.552	10179
R	$^3\Pi_1(v=0)$	2.604	10598
S	$^3\Pi_0(v=1)$	2.623	10751
T	$^3\Pi_1(v=1)$	2.672	11147
U	$^3\Pi_0(v=2)$	2.693	11316
V	$^5\Sigma^+(v=0)$	2.727	11590

[a]Two possibilities for the assignment of peaks C, D, and F–M exist; the alternative explanation is given in square brackets (see Sec. IV G).
[b]The assignment for these peaks is tentative.

lated to be 677 cm^{-1} by Froese–Fischer;[24] by using methods described by Lefebvre–Brion and Field[25] the splittings of several electronic states of the oxide can be estimated as multiples of this parameter ζ. Table III lists these estimates in terms of ζ, their values in cm^{-1}, and the observed values from the analysis of the spectrum to be presented below. The values observed for the $^5\Pi$ and $^3\Delta$ states are very close to the estimates. The difference between the estimated and observed $^3\Pi$ state splitting is somewhat larger; however, three distinct $^3\Pi$ states derive from the configuration listed in Table I, making it impossible to estimate the spin–orbit splitting without more information about the nature of the $^3\Pi$ state. The estimate provided in Table III is based on a high-spin coupling of the 2δ and 6π electrons, which is then low-spin coupled to the 12σ electron. Any mixing of this wave-

TABLE III. Spin orbit splitting parameters of MoO$^-$ and MoO in terms of the atomic molybdenum $4d$ splitting ζ (677 cm^{-1}).

Electronic state	Calculated splitting in units of ζ	Estimated splitting (cm^{-1})	Observed splitting (cm^{-1})
MoO$^-$ $X\ ^4\Pi$	$\zeta/3$	226	
MoO $X\ ^5\Pi$	$\zeta/4$	169	170
MoO $^3\Delta$	$-\zeta$	-677	$[-720]^a$
MoO $^3\Pi$	$5\zeta/12$	282	410

[a]Observation of the $^3\Delta$ spin orbit splitting is dependent on the choice of spectral interpretations indicated in Table II and in Sec. IV G.

TABLE IV. Parameters assigned for MoO^- and MoO: term energies (T_0), harmonic vibrational frequencies (ω_e), equilibrium bond lengths (r_e), and spin orbit level splittings (A).

Electronic state		Parameter	Notes
MoO^-	$X\ ^4\Pi_{-1/2}$	$\omega_e = 810(40)\ cm^{-1}$	$r_e(MoO\ X\ ^5\Pi) + 0.02$ Å
		$r_e = 1.72$ Å	
MoO	$X\ ^5\Pi$	$\omega_e = 893.5\ cm^{-1}$	From Ref. 9
		$r_e = 1.70$ Å	From Ref. 4
		$A = 169(30)\ cm^{-1}$	
	$^3\Delta$	$T_0 = 621(50)\ cm^{-1}$	Tentative assignment; see Table II and Sec. IV G
		$\omega_e = 1000(20)\ cm^{-1}$	
		$r_e = 1.63$ Å	$r_e(MoO^-\ X\ ^4\Pi) - 0.09$ Å
		$A = -720(20)\ cm^{-1}$	Tentative assignment; see Table II and Sec. IV G
	$^5\Sigma^-$	$T_0 = 8000(500)\ cm^{-1}$	Tentative assignment; see the text.
	$^3\Pi$	$T_0 = 10\ 179(20)\ cm^{-1}$	
		$\omega_e = 600(20)\ cm^{-1}$	
		$r_e = 1.66$ Å	$r_e(MoO^-\ X\ ^4\Pi) - 0.06$ Å
		$A = 410(20)\ cm^{-1}$	
	$^5\Sigma^+$	$T_0 = 11\ 590(60)\ cm^{-1}$	See also Ref. 4

function with the other two $^3\Pi$ wave functions will lead to a discrepancy between the estimated and observed spin–orbit intervals.

E. The $^5\Pi$ state

Figure 3 shows the portion of the MoO^- photoelectron spectrum from 1.0 to 2.0 eV binding energy. The peak labels in Fig. 3 correspond to those in Table II. Peaks A–C, A′, and E are assigned as transitions to the $^5\Pi$ state of MoO. The intensity ratio of peak A to peak A′ is typical for a vibrational origin to hot band intensity distribution at thermal source conditions and therefore the spacing between these peaks provides a determination of the anion vibrational frequency, $810(20)\ cm^{-1}$. Peaks A–C are regularly spaced by $169\ cm^{-1}$, indicating that the same molecular property is manifested in the spacing between peaks A and B and between B and C. Assuming such a common basis for the appearance of peaks A–C, three possibilities must be considered for their assignment: (1) they could arise from vibrational sequence bands, where the anion vibrational frequency is $169\ cm^{-1}$ smaller than that of the MoO $^5\Pi$ state; (2) a set of spin–orbit sequence bands may be responsible for these peaks, where, in analogy to the vibrational sequence, the anion spin–orbit splitting is $169\ cm^{-1}$ smaller than the $^5\Pi$ state spin–orbit splitting; or (3) these peaks correspond to a series of spin orbit levels of the $^5\Pi$ state, where the transitions originate in only one spin–orbit level of the anion. The first possibility would require significant population in the $v = 1$ and $v = 2$ states of the anion, which is inconsistent with the relative intensities of peaks A and A′. The second possibility is contradicted by the relative magnitudes of the spin orbit estimates in Table III, where the anion splitting is larger, not smaller, than the $^5\Pi$ state splitting. However, the spacing between peaks A, B, and C is consistent with the spin orbit estimate for the $^5\Pi$ state (Table III), making the third possibility, where these peaks form a spin–orbit state progression within the vibrational origin, the only

one consistent with all expectations. Thus we obtain a $^5\Pi$ state spin orbit splitting of $169(30)\ cm^{-1}$. The separation between peak A and peak E, $960(80)\ cm^{-1}$, is consistent with the known[9] vibrational frequency of the $X\ ^5\Pi$ state of MoO, $893.5\ cm^{-1}$. This provides a firm assignment for peak E, one also consistent with the angular distribution data discussed in Sec. IV C. The positions and intensities of peaks A–C and E are inconsistent with any interpretation other than the one presented here, and so the assignments for these peaks are unambiguous.

The assignment presented above does not, however, account for the remaining peaks in Fig. 3. Peak D, in particular, is not attributable to the $^5\Pi$ state and another electronic state must be invoked to account for it. All of these peaks (D and F–M) will be assigned to the $^3\Delta$ state; the details of these assignments will be presented in Sec. IV G.

The equilibrium bond length (r_e) of the MoO $X\ ^5\Pi$ state has been estimated[4] as 1.70 Å. This value can be used with a bond length change between the anion and neutral ground states, estimated by performing a Franck–Condon simulation, to obtain an approximation to r_e in the MoO^- $X\ ^4\Pi$ state. Such a simulation results in a bond length change of ±0.02 Å; we choose the positive value because the anion bond length (1.74 Å) calculated by Brocławik[12] is greater than the MoO $X\ ^5\Pi$ state bond length calculated by the same method (1.73 Å).[3] Table IV includes the resulting estimate of the anion r_e, this was used in additional Franck–Condon simulations to obtain estimates of the MoO $^3\Pi$ and $^3\Delta$ state bond lengths. Also included in Table IV is the spin orbit splitting parameter for the $X\ ^5\Pi$ state.

F. The $^3\Pi$ state

Figure 4 illustrates the higher binding energy portion of the MoO^- photoelectron spectrum, between 2.0 and 3.0 eV binding energy. The prominent progression formed by peaks Q–U and Q′ is assigned as transitions to the $^3\Pi$ state based on the analysis given below.

A spin orbit splitting and a vibrational frequency for the $^3\Pi$ state can be assigned by inspection of the relative positions and intensities of peaks Q–U in Fig. 4 and Table II. No shoulders or separate peaks appear at lower binding energy than the largest, origin peak, with the exception of a small vibrational hot band (peak Q′ in Fig. 4) separated from the origin by 810 cm^{-1}. The spacing between peaks Q and Q′ is identical to the spacing between peaks A and A′ (Fig. 3), as are their relative intensities, confirming the anion vibrational frequency assignment. Peaks Q, S, and U are spaced 600 cm^{-1} apart and have relative intensities characteristic of a Franck–Condon progression, motivating the assignment of these peaks as a vibrational progression in the MoO $^3\Pi_0$ state. The peaks labeled R and T in Fig. 3 are also separated from one another by 600 cm^{-1} and can be assigned as transitions to the $^3\Pi_1$ state; therefore the separation between the $^3\Pi$ spin orbit states, given by the spacing between peaks Q and R, is assigned as 410 cm^{-1}. Transitions to the $^3\Pi_2$ state are very weak and not observed.

This interpretation, where peaks Q–U all correspond to transitions to the $^3\Pi$ state, requires a surprisingly small vibrational frequency for this state (600 cm^{-1}) relative to calculations ($\sim$1000 cm^{-1});[2,3,10,11] however, all peaks in this region are assignable with this interpretation. Assignments using higher vibrational frequencies have been attempted, but they invariably leave at least two peaks unassigned. The only possible assignment for these two (or more) peaks is to distinct electronic states of MoO which have not been observed experimentally[4] or calculated.[2,3,10,11] The assignment using a vibrational frequency of 600 cm^{-1}, therefore, is the most economical interpretation of the positions and intensities of peaks Q–U, and the one we adopt.

A Franck–Condon simulation of the MoO $^3\Pi$ state has been performed using the equilibrium bond length determined for the MoO$^-$ $X\,^4\Pi$ state from the $^5\Pi$ state simulation described above. In this case the bond length changes by ±0.06 Å between the anion and the $^3\Pi$ state; the negative value is chosen to be consistent with trends for this state found in calculations.[2] The resulting bond length of the $^3\Pi$ state is included in Table IV along with the other parameters determined for the $^3\Pi$ state: term energy, vibrational frequency, and spin–orbit splitting parameter.

G. The $^3\Delta$ state

The nine peaks labeled D and F–M in Fig. 3 appear at binding energies inconsistent with transitions to the $^5\Pi$ state. We have identified two possibilities for the assignment of these peaks, both involving transitions to the $^3\Delta$ state, based on the following observations: (1) The first excited state of MoO, according to calculations,[2,3] is the $^3\Delta$ state, with a term energy between 2193 and 3265 cm^{-1} in the latest calculation[3] and, except for Σ states, no other electronic states appear in the calculations below the $^3\Pi$ state; (2) The fact that peaks F–M appear as pairs of peaks strongly motivates their assignment as transitions to several vibrations within two spin orbit levels of the same electronic state, eliminating the possibility that they result from transitions to

a Σ state; (3) The estimate of the splitting between the $^3\Delta$ spin orbit levels, −677 cm^{-1} (Table III), closely matches the binding energy difference (720 cm^{-1}) between each pair of peaks in the series F–M; and (4) The spacing between every other peak (i.e., F and H, G and I, etc.) of 1000 cm^{-1} agrees with the vibrational frequency predicted by the latest, density functional calculations,[3] a particular strength of this type of calculation. Thus the positions and intensities of peaks F–M are completely consistent with their assignment as transitions to the $^3\Delta$ state. However, peak D, although listed in the table as the transition to the $^3\Delta_3(v = 0)$ level, is actually displaced to 100 cm^{-1} higher binding energy than expected. Furthermore, no peak appears where the transition to the $^3\Delta_3(v = 0)$ level would normally be expected. The 100 cm^{-1} shift could be explained in at least two ways: (1) the origin of the $^3\Delta_3$ state may be perturbed by the presence of the $^5\Pi$ state and/or a low-lying Σ state; or (2) transitions to the $^3\Sigma^-$ state, calculated[3] to lie only slightly above the $^3\Delta$ state at 4025–5510 cm^{-1}, may produce peak D, raising the possibility that the states are actually reversed. In the latter case the assignment of peaks F–M may require adjustment, though even then the transitions are almost certainly to the $^3\Delta$ state. The simplest interpretation is the first, and the one we adopt.

However, the transitions which give rise to these peaks are ambiguous even given this assignment. The spin orbit levels in the $^3\Delta$ state are expected to be inverted so that the $^3\Delta_3$ level is lowest in energy, and the term energy of this level, only a few hundred wave numbers relative to the $^5\Pi_{-1}$ level, is very close to that of the $^5\Pi_3$ level. Since the total angular momentum present in the $^5\Pi_3$ and $^3\Delta_3$ levels is the same, the two states could interact very strongly, resulting in a mixed state containing levels associated with peaks D and F–M.[26] A simple calculation of the expected perturbation has been performed in the following way: the spin–orbit matrix element which connects the two states was estimated as 677 cm^{-1} (confirming that the perturbation is significant); then this was multiplied by the Franck–Condon overlaps between the vibrational levels of the unperturbed states (obtained by assuming independent Morse oscillators with ω_e and r_e for each state from Table IV) to obtain off-diagonal matrix elements with a basis set of the unperturbed levels. The term energy of the $^3\Delta_3$ level and the spin–orbit matrix element were then adjusted to match the positions of peaks D and F–M (and also peak C). The optimal perturbed state energy levels result from a spin–orbit matrix element between 340 and 677 cm^{-1} and $T_0(^3\Delta_3) = 140–300$ cm^{-1}. These levels agree with the observed peak positions within the experimental resolution for the lowest binding energy peaks, and within 100 cm^{-1} for higher levels.

The perturbed state energy levels, therefore, match the observed levels remarkably well, considering the approximate nature of this calculation, and this assignment relies only on the $^3\Delta_3$ and $^5\Pi_3$ states, with no contribution from the $^3\Delta_2$ state and therefore no measured $^3\Delta$ spin orbit splitting. While the unperturbed level assignment matches more closely the positions of peaks F–M, it contains a discrepancy in the position of peak D which cannot be explained without some sort of perturbation. A more complete understanding of

this perturbation is not available from the spectral information, and the peaks probably result from a combination of the two interpretations. The assignments listed in Table II reflect this ambiguity.

The equilibrium bond length of the MoO $^3\Delta$ state can be estimated by performing a Franck–Condon simulation wherein the anion bond length is fixed to the value determined by the $^5\Pi$ state simulation. As in the $^5\Pi$ and $^3\Pi$ state simulations, the direction of bond length change cannot be determined from the simulation. The change in the $^3\Delta$ state case is ± 0.09 Å; using calculations[2,3] as a guide, we choose the negative value. This value is included in Table IV along with the other values (T_0, ω_e, and A) obtained for the $^3\Delta$ state.

H. Other states

The assignments presented above for the $^5\Pi$, $^3\Pi$, and $^3\Delta$ states account for all features in the MoO$^-$ photoelectron spectrum except peaks N–P and peak V in Fig. 4 and Table II. The last feature, peak V, does not fit in the progression of the $^3\Pi$ state but its term energy matches closely the $^5\Sigma^+$ state term energy proposed by Hamrick *et al.*;[4] on this basis peak V is assigned as a transition to the $^5\Sigma^+$ state.

Peaks N–P, separated from the $X\,^5\Pi$ state origin by approximately 8000 cm^{-1}, present a more difficult puzzle. The intensities of these peaks appear anomalous and could result from autodetachment of an excited state of the anion at the photon energy; however, the positions and intensities do not change when the MoO$^-$ photoelectron spectrum is taken at 364 nm (3.4081 eV), casting doubt on such an explanation. Orbital energy estimates of Hamrick *et al.*[4] place the $^5\Sigma^-$ state in this region ($T_0 = 7350$ cm^{-1}), making this a possible assignment for peaks N–P. The observed separation between these peaks (250 cm^{-1}) is large for such an assignment, since it requires that the spin orbit splitting is manifested through a second order perturbation; however, the significant spin orbit interactions present in the MoO system may make such a splitting possible. The assignment of peaks N–P to the $^5\Sigma^-$ state given in Table II is to be considered speculative.

V. DISCUSSION: Mo–O BONDING

The photoelectron spectrum of MoO$^-$ provides a wealth of information about the ground state and several low-lying electronic states which can be used to infer more about the physical character of the Mo–O bond. Angular distributions of photodetachment to form the $^5\Pi$ and $^3\Pi$ states strongly suggest that the extra electron in the anion is in an *s*-like orbital. The small geometry change indicated by the Franck–Condon analyses of both of these states show that the orbital is essentially nonbonding. The electron affinity measured for MoO provides further evidence for the nonbonding character of this orbital: The MoO EA(1.290 eV) is much closer to that of O(1.4611 eV)[16] than to Mo(0.748 eV). The dissociation energy of the anion, D_0(Mo–O$^-$), is to the Mo($^7S_3$)+O$^-$(^2P) asymptote; the neutral MoO molecule dissociates to the Mo($^7S_3$)+O(^3P) asymptote. The energy difference between these asymptotes is EA(O), while, by

definition, the energy difference between the MoO and MoO$^-$ ground rovibrational states is EA(MoO). A simple thermodynamic rule results

$$D_0(\text{MoO}^-) + \text{EA(O)} = \text{EA(MoO)} + D_0(\text{MoO}).$$

Since EA(MoO)$\approx$EA(O), the dissociation energies must also be approximately equal. This is further evidence that the extra electron in the anion is inserted in a nonbonding orbital.

The MoO molecular orbital energies have been estimated by Hamrick *et al.*,[4] and the term energies of the MoO $^3\Pi$, $^5\Sigma^+$, and $^5\Sigma^-$ electronic states observed in the MoO$^-$ photoelectron spectrum support these estimates. This confluence of the experimental results provides strong evidence that the orbital energies have been well characterized to the extent that they can be considered independent of electron–electron repulsion and configuration interaction.

The term energy of the $^3\Delta$ state, however, has apparently been consistently overestimated by calculations[2,3,10,11] (which have been, until this report, the only way to examine this state). Since the formation of this state involves moving an electron from the MoO 6π orbital to an already singly occupied 2δ orbital, the term energy is not simply determined by the relative orbital energies but by a balance of these energy differences with the electron–electron repulsion energy introduced by doubly occupying a 2δ orbital, making the (hopefully temporary) intractability of this problem unsurprising.

VI. CONCLUSIONS

The photoelectron spectra of Mo$^-$ and MoO$^-$ have been examined. The electron affinity of Mo has been measured as 0.748(2) eV. The focus of this project is on the MoO$^-$ spectrum, and the analysis of this spectrum has led to the extraction of a number of previously unobserved properties of MoO and MoO$^-$, summarized in Table III. The degree of confidence which can be placed in these measurements varies; firm assignments include the adiabatic EA of MoO, relative energies of the MoO$^-$ $X\,^4\Pi_{-1/2}$, MoO $X\,^5\Pi_\Omega$ ($\Omega=-1,0,1$), MoO $^3\Pi_\Omega$ ($\Omega=0,1$), and MoO $^5\Sigma^+$ electronic states, and the vibrational frequencies of the MoO$^-$ $X\,^4\Pi_{-1/2}$ and MoO $^3\Pi$ states. The term energy, spin orbit splitting, and vibrational frequency of the MoO $^3\Delta$ state are tentatively assigned, and an estimate of the MoO $^5\Sigma^-$ term energy is given.

The photoelectron spectrum of MoO$^-$ has yielded a wealth of new information about a molecule which, though it is only a diatomic, is surprisingly poorly understood. Many of the conclusions drawn from previous studies are strongly supported by evidence in the MoO$^-$ photoelectron spectrum; however, many questions remain about the MoO system. The most prominent example is the position of the $^3\Delta$ state, where the term energy presented in this report deviates from calculations, and the lowest $^3\Delta$ vibrational and spin orbit state (peak D, Fig. 3 and Table II) appears to be strongly perturbed. Any further understanding of this and other puzzles which may be gained through more experimental

and theoretical investigations will significantly extend understanding of molybdenum monoxide, and of high electron spin environments in general.

ACKNOWLEDGMENTS

[1] A. J. Merer, Annu. Rev. Phys. Chem. **40**, 407 (1989).
[2] S. R. Langhoff, C. W. Bauschlicher, L. G. M. Pettersson, and P. E. M. Siegbahn, Chem. Phys. **132**, 49 (1989).
[3] E. Brocławik and D. R. Salahub, Int. J. Quantum Chem. **52**, 1017 (1994).
[4] Y. M. Hamrick, S. Taylor, and M. D. Morse, J. Mol. Spectrosc. **146**, 274 (1991).
[5] G. Picardi, Atti Accad. Lincei **17**, 654 (1933).
[6] A. Gatterer, J. Junkes, E. W. Salpeter, and B. Rosen, *Molecular Spectra of Metallic Oxides* (Specola Vaticana, Vatican City, 1957).
[7] J. C. Howard and J. G. Conway, J. Chem. Phys. **43**, 3055 (1965).
[8] K. P. Huber and G. Herzberg, *Constants of Diatomic Molecules* (Van Nostrand Reinhold, New York, 1979).
[9] J. K. Bates and D. M. Gruen, J. Mol. Spectrosc. **78**, 284 (1979).
[10] C. W. Bauschlicher, C. J. Nelin, and P. S. Bagus, J. Chem. Phys. **82**, 3265 (1985).
[11] C. J. Nelin and C. W. Bauschlicher, Chem. Phys. Lett. **118**, 221 (1985).
[12] E. Brocławik (private communication, 1995).
[13] K. M. Ervin, J. Ho, and W. C. Lineberger, J. Chem. Phys. **91**, 5974 (1989).
[14] D. G. Leopold, K. K. Murray, A. E. Stevens-Miller, and W. C. Lineberger, J. Chem. Phys. **83**, 4849 (1985).
[15] K. M. Ervin and W. C. Lineberger, in *Advances in Gas Phase Ion Chemistry*, edited by N. G. Adams and L. M. Babcock (JAI, Greenwich, 1992), Vol. 1, p. 121.
[16] D. M. Neumark, K. R. Lykke, T. Andersen, and W. C. Lineberger, Phys. Rev. A **32**, 1890 (1985).
[17] C. E. Moore, *Atomic Energy Levels* (US GPO Circular No. 467, Washington, DC, 1952).
[18] C. S. Feigerle, R. R. Corderman, S. V. Bobashev, and W. C. Lineberger, J. Chem. Phys. **74**, 1580 (1981).
[19] J. Cooper and R. N. Zare, J. Chem. Phys. **48**, 942 (1968).
[20] J. Cooper and R. N. Zare, J. Chem. Phys. **49**, 4252 (1968).
[21] J. L. Hall and M. W. Siegel, J. Chem. Phys. **48**, 943 (1968).
[22] D. Hanstorp, C. Bengtsson, and D. J. Larson, Phys. Rev. A **40**, 670 (1989).
[23] M. Blume and R. E. Watson, Proc. R. Soc. London, Ser. A **270**, 127 (1960).
[24] C. Froese-Fischer, *The Hartree–Fock Method for Atoms. A Numerical Approach* (Wiley, New York, 1977).
[25] H. Lefebvre-Brion and R. W. Field, *Perturbations in the Spectra of Diatomic Molecules* (Academic, Orlando, 1986).
[26] The authors would like to thank the reviewer of this article for suggesting the alternative interpretation for peaks D and F–M presented here.